ELSEVIER

Brain Research 785 (1998) 114–128

BRAIN RESEARCH

Research report

The differential distribution of AMPA-receptor subunits in the tectofugal system of the pigeon

Carsten Theiss *, Burkhard Hellmann, Onur Güntürkün

Biopsychologie, Ruhr-Universität Bochum, D-44780 Bochum, Germany

Accepted 11 November 1997

Abstract

The tectofugal system of the pigeon was examined for the distribution of several glutamate-receptor subunits (AMPA Glu R1, Glu R2/3, Glu R4) and the calcium binding protein parvalbumin. With respect to the different antigens, a heterogeneous distribution was observed. Within the optic tectum, the Glu R1 like immunoreactivity was limited to the layers 2–5, 9, 10, and sparsely in layer 13, whereas the antibody to Glu R2/3 stained cell bodies in layers 9, 10, and very heavily in layer 13. In the rotundus only the Glu R4 antigen was expressed, while within the ectostriatal complex a large number of Glu R2/3 and a smaller contingent of Glu R4 positive neurons were stained. Quantitative analysis proved significant heterogeneities of these antigens in the mesencephalic as well as the diencephalic centre of the tectofugal pathway. The number of Glu R2/3 positive neurons undergoes a two-fold increase from the dorsal to the ventral lamina 13 of the optic tectum. Alterations in the amount of immunoreactive neurons were also observed within the rotundus, since the number of Glu R4 positive cells decreased from dorsal to ventral. Morphological differences and their correlation with functional specializations in visual information processing are discussed. © 1998 Elsevier Science B.V.

Keywords: Glutamate; Parvalbumin; Immunohistochemistry; Birds; Tectum; Nucleus rotundus; Nucleus triangularis; Ectostriatum; Heterogeneity; Dorso–ventral gradient

1. Introduction

In birds visual stimuli are processed within two main ascending information streams, the thalamofugal pathway, which is comparable to the geniculocortical system of mammals, and the tectofugal pathway, which is similar to the extrageniculocortical pathway [43].

The thalamofugal pathway consists of the retinal projection onto the contralateral nucleus geniculatus lateralis pars dorsalis and the projection from this thalamic nucleus to the visual wulst in the forebrain. The tectofugal pathway, which is in the focus of this study, is composed of optic nerve axons which terminate in the contralateral optic tectum. Fibers ascend from this mesencephalic structure to the thalamic nucleus rotundus and the nucleus triangularis, which project to the telencephalic ectostriatum [42]. The used numerical nomenclature is according to Ramon y Cajal [60]. Within the tectum retinal ganglion cells terminate in a topographic manner in the superficial layers 2–7 with the highest synaptic density in layer 5 [33]. Visual information is transmitted directly by axodendritic contacts or indirectly via interneurons to multipolar neurons of layer 13 [31], which are the major source for tecto–rotundal and tecto–triangular projections [5,6,28,41,42]. Since the projection to the nucleus rotundus is bilaterally organized, this thalamic nucleus integrates input of both tecta [6,28,57]. Histochemical and electrophysiological studies revealed subdivisions within the nucleus rotundus [24,49,50,55,65,82]. The rotundus projects topographically to the ectostriatal core in the forebrain, from where axons ascend into the surrounding ectostriatal belt [5].

In pigeons, the tectofugal pathway is more prominent than the thalamofugal pathway, and lesion experiments have shown that this ascending system subserves various

Abbreviations: ABC: avidin–biotin-conjugate; ACh E: acetylcholineesterase; AMPA: α-amino-3-hydroxy-5-methyl-isoaxazole propionic acid; Ca^{2+}: Calcium; DAB: 3,3′-diaminobenzidine; E: ectostriatum; HRP: horseradish peroxidase; NMDA: *N*-methyl-D-aspartate; PBS: phosphate-buffered saline; PV: parvalbumin; RT: nucleus rotundus; T: nucleus triangularis; TO: optic tectum

* Corresponding author. AE Biopsychologie, Fakultät für Psychologie, Ruhr-Universität Bochum, D-44780 Bochum, Germany. Fax: +49-0-234-7094377; E-mail: carsten.theiss@rz.ruhr.uni.bochum.de

aspects of vision, like luminance, colour and movement discriminations [27]. The understanding of the biochemical organization of the tectofugal pathway is far from complete. Up to now it is even unclear, which neurotransmitters are responsible for excitatory signal transmission within this system. Autoradiographic ligand-binding studies suggest tectally projecting retinal ganglion cells to utilize the excitatory neurotransmitter glutamate [4,35,36]. Moreover high levels of neuronal long-time activity, as demonstrated by histochemical cytochrome-oxidase-activity at different levels of the tectofugal pathway, indicate the existence of strong excitatory input to structures of the tectofugal system [9,34]. Glutamate is suggested to be one of the major excitatory neurotransmitters in the vertebrate brain [52,53]. Corresponding glutamate-receptors can be subdivided into G-protein coupled metabotrophic receptors [75,76], and ionotropic glutamate-receptors [21,51,84]. Three different ionotropic glutamate-receptors, which are built of receptor subunits in a pentameric structure, can be distinguished according to pharmacological studies: NMDA-(*N*-methyl-D-aspartate) receptors, kainate-receptors, and AMPA-(α-amino-3-hydroxy-5-methyl-isoaxazole propionic acid) receptors [21,51,84]. The receptor subunits Glu R1, Glu R2, Glu R3, and Glu R4, for which AMPA is the most potent specific agonist, form homomeric or heteromeric receptors, with Glu R2 determining the Ca^{2+}-permeability [8,38,44].

In the present study, the immunohistochemical localisation of Glu R1, Glu R2/3 and Glu R4 in the tectofugal system of the pigeon is described, using antibodies against C-terminal amino acid sequences of Glu R1 to Glu R4. The antibody used for this study marked Glu R2 as well as Glu R3 likewise. According to the fact that the receptor subunit Glu R2 determines the calcium-permeability of the functional glutamate-receptor, we additionally performed double-labeling experiments with an antibody to the calcium-binding protein parvalbumin (PV).

2. Materials and methods

2.1. Antibodies

The polyclonal rabbit-antibodies utilized during the present study were directed against synthesized oligopeptides of C-terminal amino acid sequences of the rat AMPA-receptor subunits Glu R1, Glu R2/3, and Glu R4 (Chemicon, Temecula, USA). The peptide sequences used to generate these antibodies were identical between pigeon and rat [58], and previous studies showed that the AMPA-receptor subunit antibodies recognize AMPA-receptors in the chick brain [72,73]. The monoclonal mouse-antibody against PV (Sigma-Aldrich Chemie, Deisenhofen, Germany) specifically recognizes the first Ca^{2+}-bound form of this protein [12,77].

2.2. Tissue preparation

Ten unsexed adult pigeons (*Columba livia*, 1 to 10 yr old), from local stock, were injected with 1000 IU heparin 20 min before perfusion and anesthetized with equithesin (0.4 ml/100 mg body weight). The animals were perfused transcardially with about 400 ml 0.9% NaCl (40°C), followed by 1000 ml ice-cold fixative consisting of 4% paraformaldehyde in 0.12 M phosphate buffer (PBS, pH 7.4) for PV-immunohistochemistry, or of the fixative with the addition of 0.2% glutaraldehyde for glutamate-immunohistochemistry, respectively. The brains were removed and post-fixed in the same fixative to which 30% sucrose was added. The post-fixation times was 1 h for PV, and 16 h for glutamate receptor-immunohistochemistry at 4°C. Brains were then stored in PBS with 30% sucrose for 24 h at 4°C for cryoprotection. Frontal sections were cut at 30 μm with a freezing microtome and collected free-floating in 0.12 M PBS.

2.3. DAB-immunohistochemistry

All incubations were carried out on a shaker. Sections were first placed in 0.1% H_2O_2 for 30 min to inactivate endogenous peroxidase-activity, washed three times in PBS, incubated in 10% (w/v) normal goat serum in PBS for 30 min to block non-specific binding-sites in the tissue, and then incubated in the primary antibody in PBS overnight at 4°C. Antibodies were used in a wide range of concentrations, but most common as a concentration of 1/500 (diluted in 0.12 M PBS + 0.3% (v/v) Triton-X) for all of them. Following thorough washing in PBS the brain-slices were incubated in the secondary antibody solution (Vector biotinylated IgG goat-anti-mouse or goat-anti-rabbit antibodies [Burlingame, CA, USA], 1/200 diluted in PBS + 0.3% Triton-X). After three further washes a conventional ABC-peroxidase (Vector Elite-kit) and heavy metal intensified DAB reaction, according to Adams [2] and Shu [74], was performed. Finally, slices were washed in PBS, mounted, dehydrated and coverslipped. To estimate the percentage of Glu R2/3 and Glu R4 positive neurons, nissl-stained slices were made with cresyl violet.

2.4. Indirect immunofluorescence procedure

As the fixation protocol for histochemical procedures for the demonstration of AMPA-receptor subunits and PV varied to an important extent, in our double-labeling experiments we utilized a compromise of the different fixation protocols, resulting in a reduction of signal to noise ratio for both antigens. This ratio was additionally diminished by the limited signal amplification of the indirect immunofluorescence method in comparison to the biotin–peroxidase technique. Despite these limitations, the results of

the co-localisation experiments of Glu R2/3, Glu R4 and parvalbumin revealed clear differences in the extend of double-labeling within distinct structures of the tectofugal system.

Tissue preparation varied from the protocol used for the detection of AMPA-receptor subunits, in that post-fixation times ranged between 2 and 3 h.

Slices were incubated overnight at 4°C in the PV-primary antibody (1/100) in PBS with 0.3% (v/v) Triton-X. Afterwards slices were washed three times (per 10 min) in PBS, pre-incubated in 10% (w/v) bovine serum albumin, and then washed three additional times. Slices were then incubated for 1 h with Texas Red TRSC labeled donkey antibody (1/200) directed against mouse IgG (Jackson, Dianova, Hamburg, Germany) and the reaction was stopped by three washes in PBS. This procedure was repeated for the second primary antibodies, Glu R2/3 or Glu R4 (both 1/500), but in this cases the following modification was used to amplify the immunosignal: instead of the respective fluorescence dye-coupled secondary antibody, a biotinylated secondary antibody (1/200) directed against mouse IgG from sheep (Vector) was used. Slices were then incubated in avidin-coupled fluoresceine (avidin DCS; Vector) for 1 h, followed by incubation in a biotinylated tertiary antibody (1/100) directed against avidin (anti-avidin D; Vector) for 1 h, and again fluoresceine avidin DCS for 1 h. All these steps were carried out in PBS with Triton-X omitted, and were separated by three washes in PBS of 10 min each. Slices were mounted and coverslipped with Elvanol.

For immunofluorescence the following filters were used: Olympus BH-IB block with additional short-pass emitter filter G520 (FITC). Chroma exciter HQ 577/10 with dichromic beamsplitter Q 585 LP and emitter HQ 645/75 (TRSC).

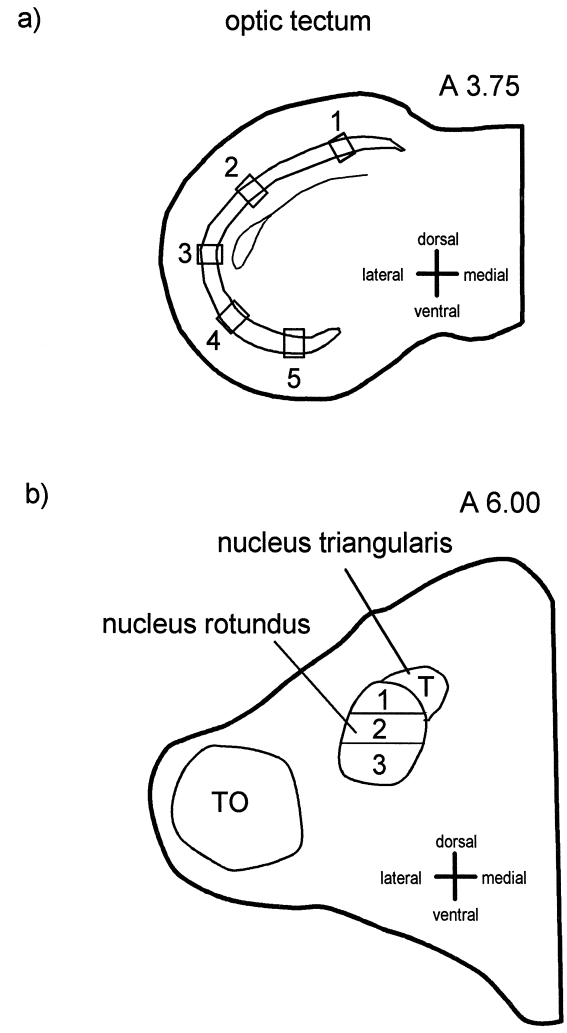

Fig. 1. Schematic reconstruction of one tectal hemisphere (a) and the nuclei rotundus and triangularis (b). Boxes indicate the location of areas in which cell countings were performed. Anteroposterior coordinates are indicated according to the pigeon brain atlas [40].

2.5. Qualitative analysis

The qualitative cell number analysis was performed for the optic tectum, the nucleus rotundus and the ectostriatum with an 'Olympus BH-2' microscope, connected via a video-camera to an image-analysing system (SIS, Münster, Germany).

2.6. Quantitative analysis in the optic tectum

A quantitative cell number analysis was performed for neurons within layer 13 of the optic tectum. Therefore, the frontal plane of this layer was divided into five subdivisions of equal length from ventral to dorsal named field TO 1 to field TO 5 (Fig. 1a). In frames of identical size ($270 \times 220 \times 30$ μm) within these fields AMPA-receptor positive neurons were counted over an extension of 3 mm (A 2.5–A 5.5) with the help of an image analysing system ('Analysis', SIS). The same procedure was repeated for control purposes in cresyl violet preparations. Quantitative analysis was carried out with three pigeons.

Fig. 2. Sections throughout the TO, stained against different glutamate receptor subunits and parvalbumin. Numbers indicate the location of tectal layers according to [60]. (a) Distribution of Glu R1-like immunoreactivity: The antibody stained a diffuse band in the retino-receptive layers 4–7, and cell bodies in layers 2–5, 9, and 10, as well as a few cells in layer 13. (b) Distribution of Glu R2/3 positive cells. The antibody exhibited labeling of a few neural somata in layer 10 and strong labeling of the cell bodies and proximal dendrites of a large number of multipolar neurons in layer 13. (c) Immunohistochemistry with Glu R4 resulted in a very light and diffuse staining of layers 2–13. (d) Parvalbumin-immunoreactive cells were observed in layers 2–4, 6, 8, and 10, with apical dendrites of layer 8 and 10 neurons stained up to the superficial layers. Bar = 250 μm.

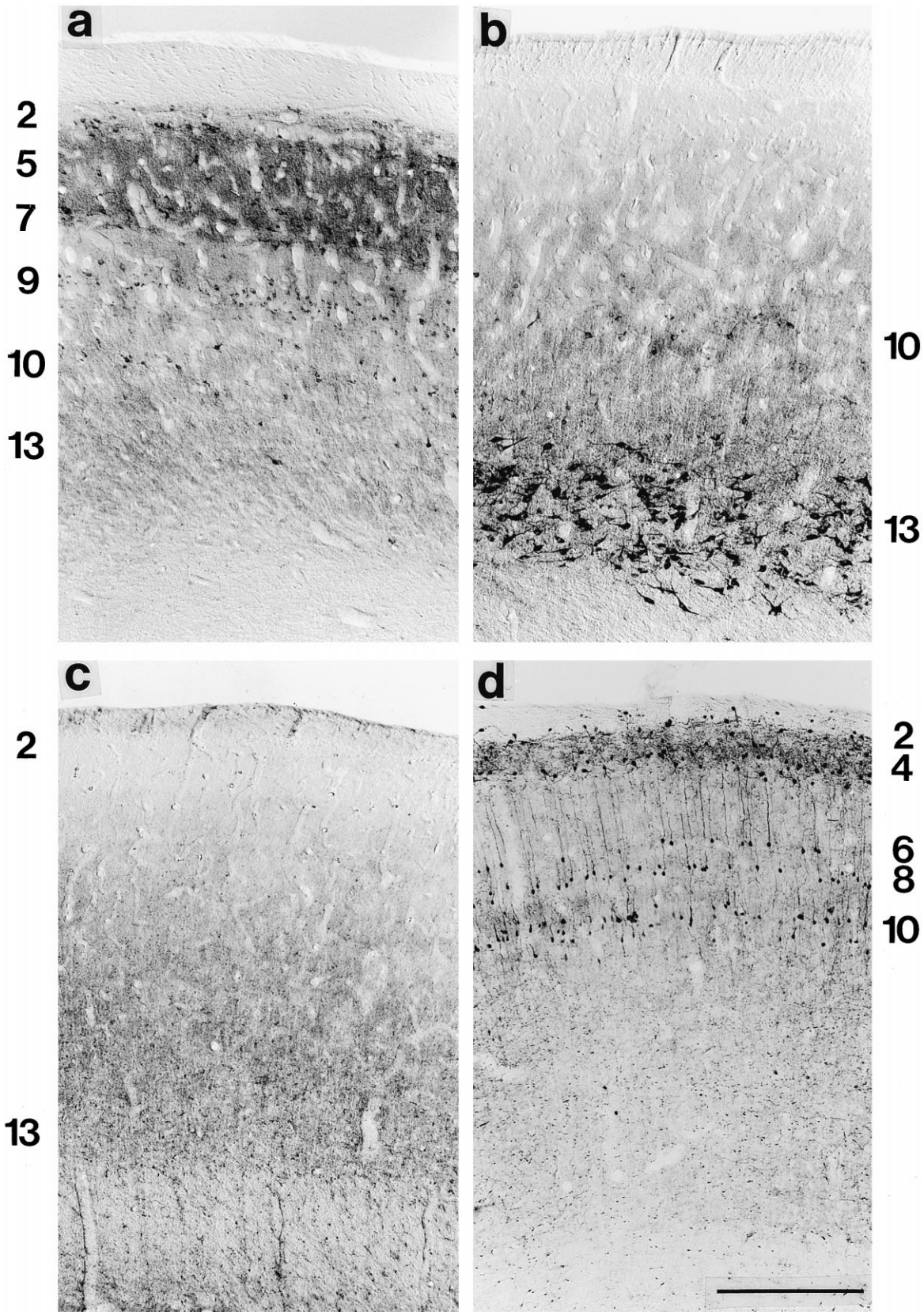
a
2
5
7
9
10
13
b
10
13
c
2
13
d
2
4
6
8
10

2.7. Quantitative analysis in the rotundus

In the nucleus rotundus the labeling pattern was also quantified, dividing the frontal plane into three subdivisions from dorsal to ventral named field RT 1 to RT 3 and an additional field in the triangularis (T) located as shown in Fig. 1b. In frames of identical size ($270 \times 220 \times 30$ μm) within these fields AMPA-receptor positive cells and cresyl violet stained neurons were counted over a caudo–rostral extension of 1 mm (A 5.5–A 6.5) as in the quantitative analysis in the TO.

3. Results

3.1. Qualitative analysis

The labeling patterns of antibodies directed against Glu R1, Glu R2/3, and Glu R4 comprised important variations. In general, Glu R1 and Glu R4 showed perikaryal and neuropil staining, while dense immunolabeling of Glu R2/3 was restricted to cell bodies and proximal dendrites. Overall staining was highest for the antibody to Glu R2/3, moderate for Glu R4 and slightly less for Glu R1. With the antibody against PV a pronounced staining of somata and dendrites was achieved. Sections in which a serum of the host of the primary antibody or PBS was substituted for primary antibodies showed no specific staining, except for a very light background staining of neurons in the nucleus rotundus.

3.2. Optic tectum

Along the tectofugal pathway a heterogeneous distribution of AMPA-receptor subunits Glu R1 to Glu R4-positive labeling was observed. Within the optic tectum, as the first level of the tectofugal system, the antibody against Glu R1 labeled cell bodies in layers 2 to 7, 9 and 10, as well as a few cells in layer 13. Additionally, a diffuse neuropil band in layers 4–7 was stained (Fig. 2a). Clearly visible cells in layers 2–5 mostly were part of the horizontally organized system with a dendritic plexus parallel to the surface of the optic tectum. Cells stained in layer 9 were radial and those in layers 10 and 13 were multipolar neurons. In contrast, the antibody to Glu R2/3 stained somata of a few multipolar cells in layer 10 and the somata and proximal dendrites of a large number of multipolar neurons in layer 13 (Fig. 2b). No Glu R4 positive cells

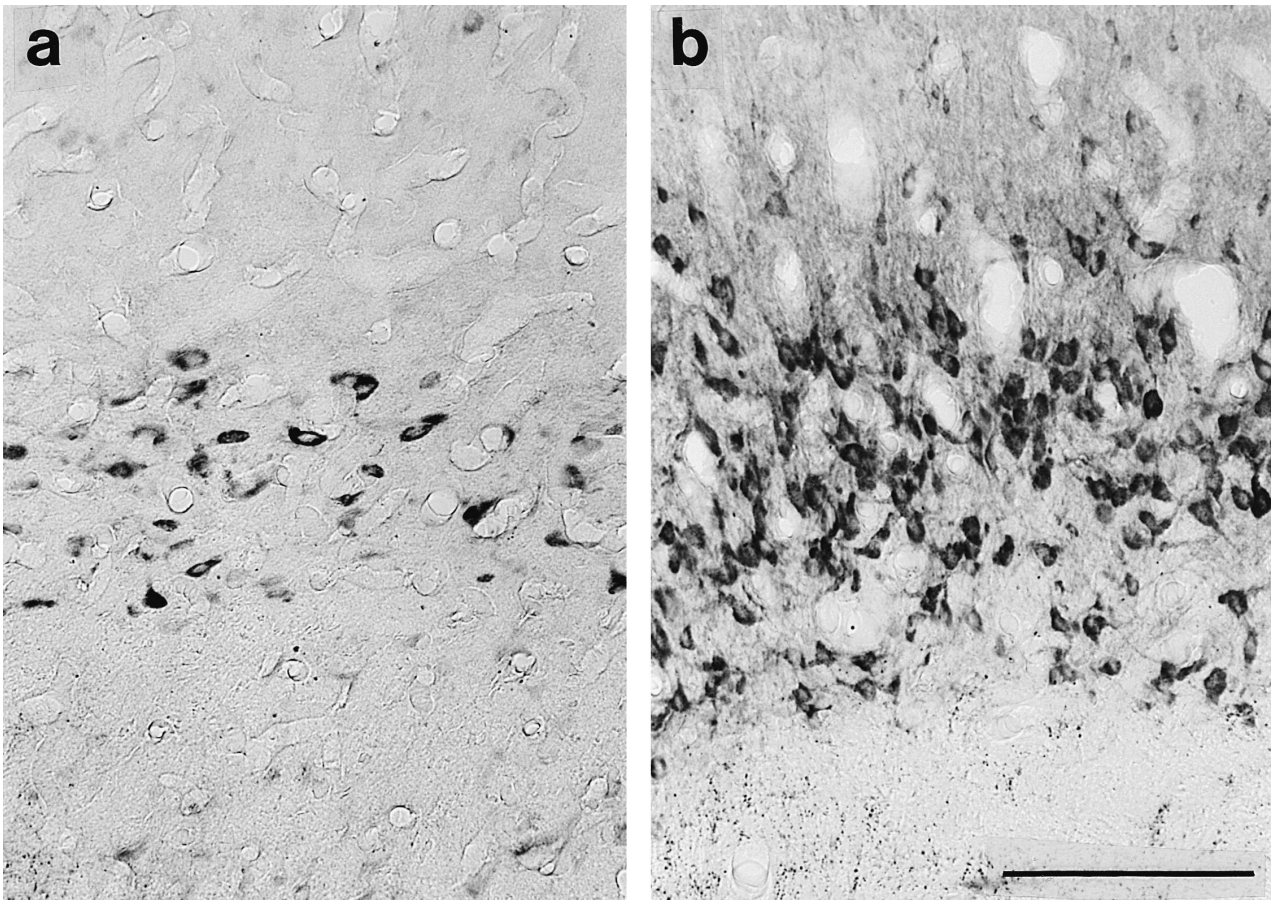

Fig. 3. Higher magnification of Glu R2/3-immunopositive cells within layer 13 of the dorsal (a) and the ventral tectum (b) within the same frontal section. Bar = 100 μm.

were found in the optic tectum, except a very light and diffuse neuropil staining in layers 2–13 (Fig. 2c). Cells immunostained for PV were clearly visible in superficial layers 2, 3, and 4, as well as in layers 6, 8, and 10 (Fig. 2d). In contrast to the glutamate-receptor immunoreactive neurons the PV-labeling stained dendrites to the finest details such that apical dendrites of cells in laminae 8 and 10 could be followed up to the superficial layers. Double-labeling experiments with antibodies against Glu R2/3 and PV revealed no neurons expressing both antigens at any place in the tectum.

The analysis of Glu R2/3 positive neurons in layer 13 of the optic tectum revealed a clearly visible dorso–ventral gradient. To quantify this difference, Glu R2/3-positive cells in layer 13 were counted in five dorsoventrally arranged fields of equal size (TO 1 to TO 5) as outlined in Section 2. These counts showed a continuous increase in labeled cell numbers from dorsal to ventral from on the

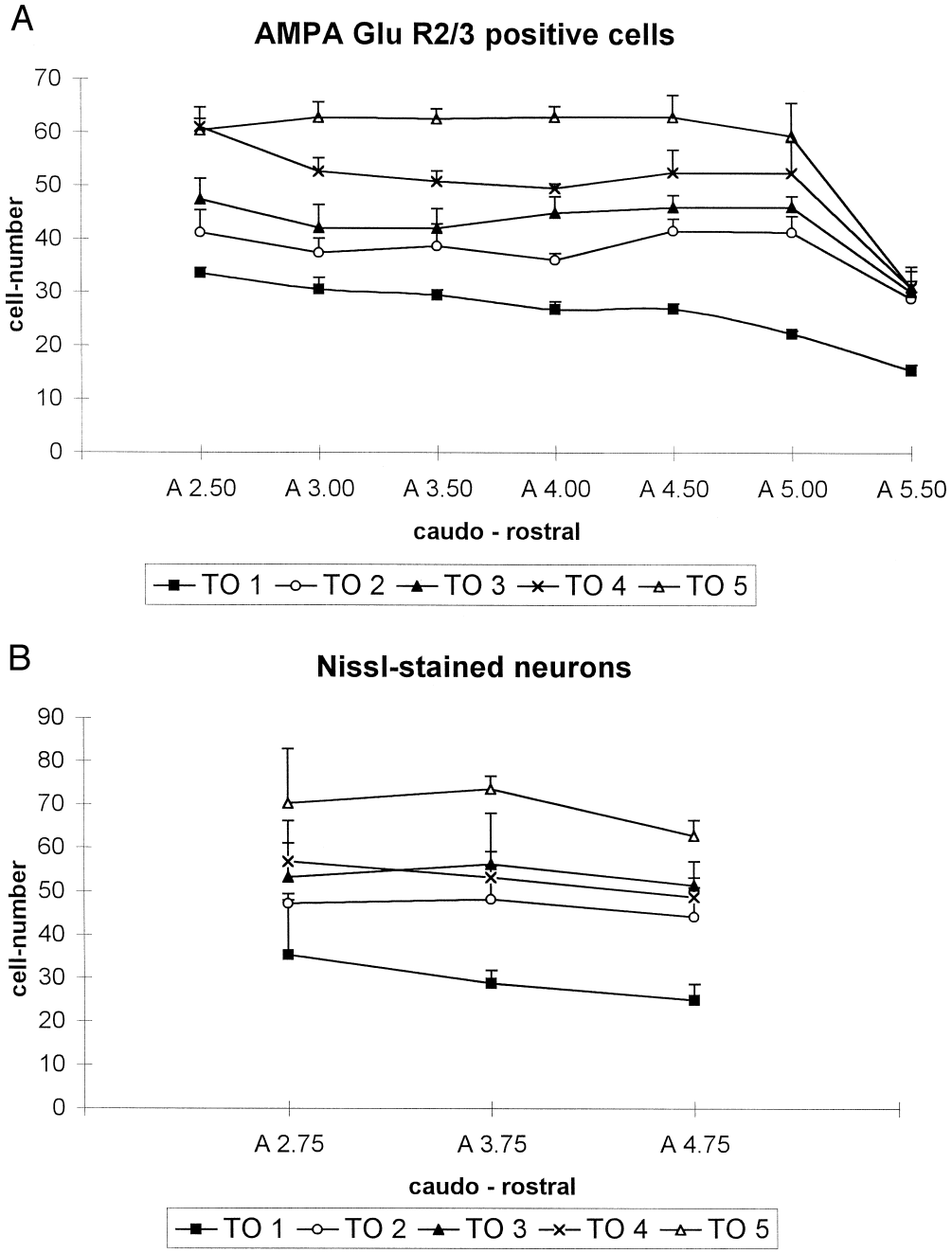

Fig. 4. The number of Glu R2/3-positive neurons (a) and nissl-stained neurons (b) in layer 13 of the optic tectum showed a continuous increase from dorsal (TO 1) to ventral (TO 5). Only at the most rostral tip of layer 13 the dorso–ventral differences were abolished. Nissl countings were performed in steps of 1 mm. Symbols indicate the mean cell number plus standard deviations.

average of 27 neurons per section in TO 1 to 59 in TO 5 (Fig. 3a,b, Fig. 4a). Since there were no detectable left–right differences or caudo–rostral variations over an extension from A 2.50 to A 5.00, the scores of both hemispheres and antero–posterior positions were pooled for statistical analysis, to calculate the average values. A Friedman test proofed the dorso–ventral variation to be significant ($n = 3$; $\chi^2 = 12.00$; $df = 4$; $p < 0.05$). A corresponding analysis in nissl-stained sections showed that this dorso–ventral gradient was not specific for Glu R2/3-like immunoreactivity but was also visible in the same extent for overall cell number. The cresyl violet cell counts revealed a continuous increase from 30 in TO 1 to 69 in TO 5 (Friedman-test, $n = 3$, $\chi^2 = 12.00$; $df = 4$; $p < 0.05$) (Fig. 4b). Only at the most rostral tip of lamina 13 (A 5.50), where the dorsoventrally arranged fields TO 1 to TO 5 virtually collapsed, the dorso–ventral difference was abolished. The increase in cell number from dorsal to ventral was not accompanied by a concomitant increase of layer thickness: TO 5 was 42.8% thicker than TO 1 while cell numbers increased with 130% (Fig. 5). Therefore, cell density also increases from dorsal to ventral within lamina 13 of the optic tectum.

To summarize the results of this quantitative analysis, the fields of measurements were drawn on the lateral view of a two dimensional reconstruction of the unfolded lamina 13 (Fig. 6). It is clearly visible that cell number increases from dorsal to ventral. The representation of the area centralis and of the red field was drawn according to Hamdi and Whitteridge [30] and Remy and Güntürkün [63]. Cell numbers do not specifically increase in these fields of enhanced vision.

3.3. Nuclei rotundus and triangularis

The antibody to Glu R4 moderately labeled cell bodies and proximal parts of stem dendrites (Fig. 7a), but no Glu R1 or Glu R2/3 positive neurons were detected. Generally neurons of various sizes and shapes were stained with Glu R4, with soma diameters ranging from 6 to 37 μm. Despite this enormous variance, which could indicate the presence of different neuron types, cell size measurements in three animals revealed an unimodal distribution with a peak at 17 μm. Additionally, a diffuse staining was visible which probably represents labeled neuropil. PV-like immunoreactivity revealed a strong somatic and diffuse neuropil labeling (Fig. 7b). The Glu R4 and PV double-labeling studies in the nuclei rotundus and triangularis disclosed a high number of co-localisations, in which all Glu R4 expressing neurons were PV positive, with a few cells showing PV but no Glu R4-like immunoreactivity (Fig. 8).

The distribution of Glu R4-positive cells in the rotundus demonstrated important regional variations with a dorso–ventral as well as an antero–posterior gradient. To analyse these regional differences in quantitative detail, three rotundal regions (RT 1 to RT 3) and an additional field in the triangularis (T) located as shown in Fig. 1b and outlined in detail in Section 2 were defined. Counts were performed in the three frontal sections A 5.50, A 6.00, and A 6.50, sections in which both nuclei are prominent. Quantitative data are given in Fig. 9. In the dorsal area RT 1 of the nucleus rotundus 61% more neurons were stained with the antibody as in ventral area RT 3 (Fig. 10); rostrally this gradient became weaker. For the statistical analysis the antero–posterior data were lumped and a

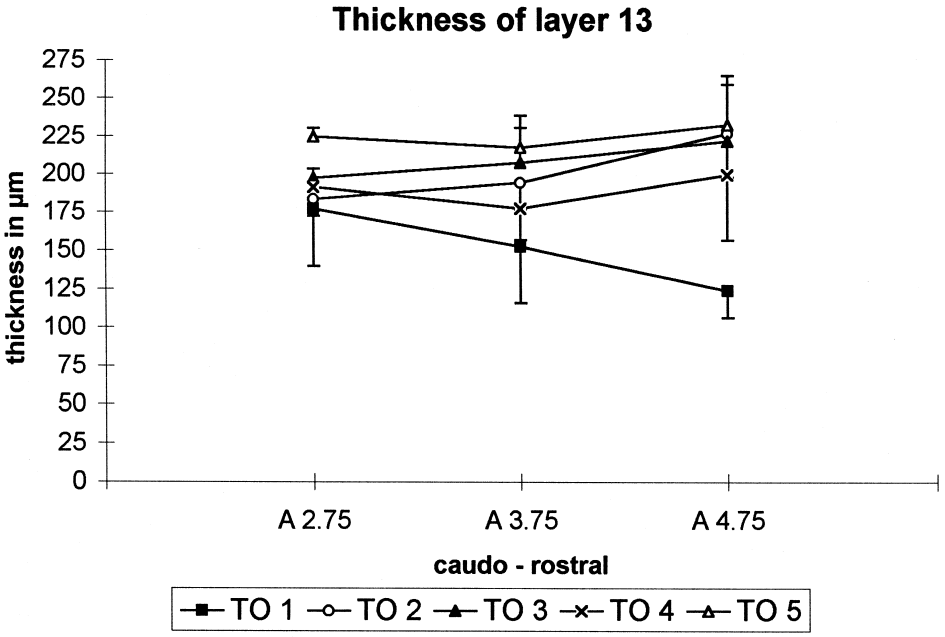

Fig. 5. The thickness of tectal layer 13 increased from dorsal (TO 1) to ventral (TO 5). Lines indicate the mean of the layer-thickness between A 2.75 and A 4.75 (coordinates according to Ref. [40]). Different symbols indicate the fields of measurement along the dorso–ventral axis of the TO.

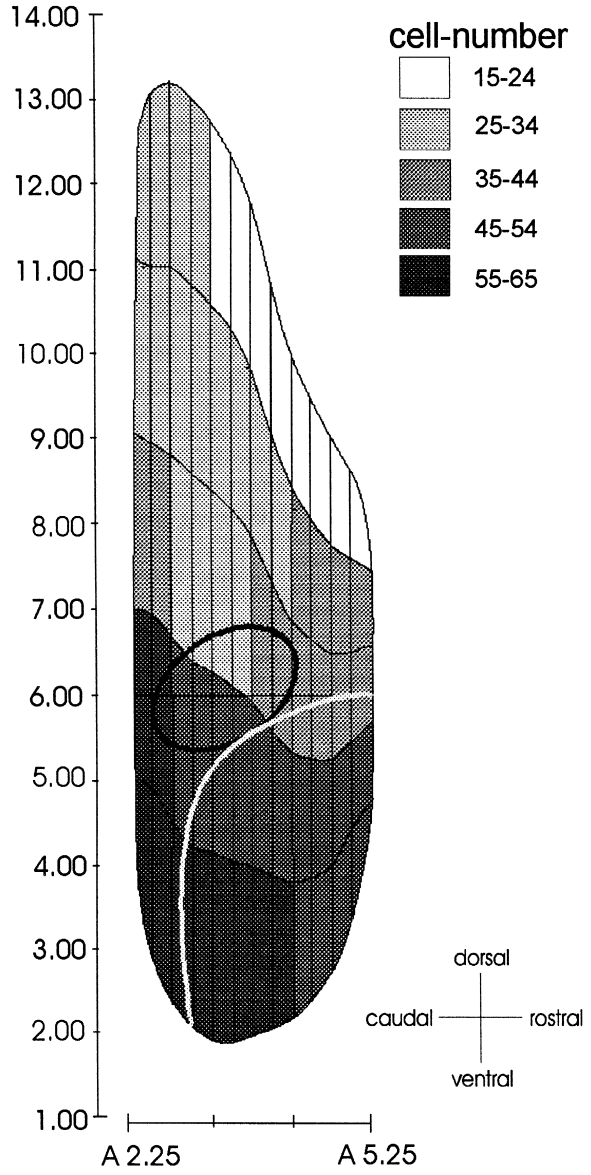

Fig. 6. Reconstruction of the cell number in layer 13 on a two dimensional map of the surface of this layer. The numbers at the bottom correspond to the anteroposterior coordinates of the atlas of the pigeon brain [40]. The numbers at the left side give the height in mm. Only the point '6' corresponds to the dorso–ventral coordinate '6' of the pigeon brain atlas. All other numbers give the topological extent of the layer 13 dorsal and ventral to this anchor point along the curvature of this layer. The increase of cell number from dorsal to ventral is reflected by the strength of gray shades. The tectal representations of the area centralis and the red field are indicated by black and white lines.

Friedman–ANOVA for non-parametric analysis was run with the three dorsoventral fields as separate levels of the repeated measures factor. The number of labeled cells significantly differed between the three fields (Friedman Test: $n = 3$; $\chi^2 = 6.00$; $df = 2$; $p < 0.05$). This differentiation was not specific for the Glu R4-stained neurons but could also be revealed with cresyl violet stained sections (Friedman Test: $n = 3$; $\chi^2 = 6.00$; $df = 2$; $p < 0.05$). To summarize, the rotundus clearly shows a dorsoventral decrease of cell density which is also reflected in the number of Glu R4-labeled neurons per standard field of measurement. This analysis, however, overshadows subtle differences in the antero–posterior plane. As visible in Fig. 9 there is additionally a slight caudo–rostral decrease in cell density in the most dorsal field RT 1. Cell numbers in triangularis were always slightly higher than in RT 1.

3.4. Ectostriatum

In the ectostriatum the antibody to Glu R2/3 labeled somata and stem dendrites of a large number of cells (Fig. 11a), whereas the antibody to Glu R4 marked only a few perikarya (Fig. 11b). A difference in the staining pattern between the ectostriatal 'belt' and 'core' could not be observed. Neurons of various sizes were stained with Glu R2/3, with soma diameters ranging from 6 to 24 μm. Cell size measurements in three animals revealed an unimodal distribution with a peak at 12 μm. No differentiation between interneurons and projection neurons could be

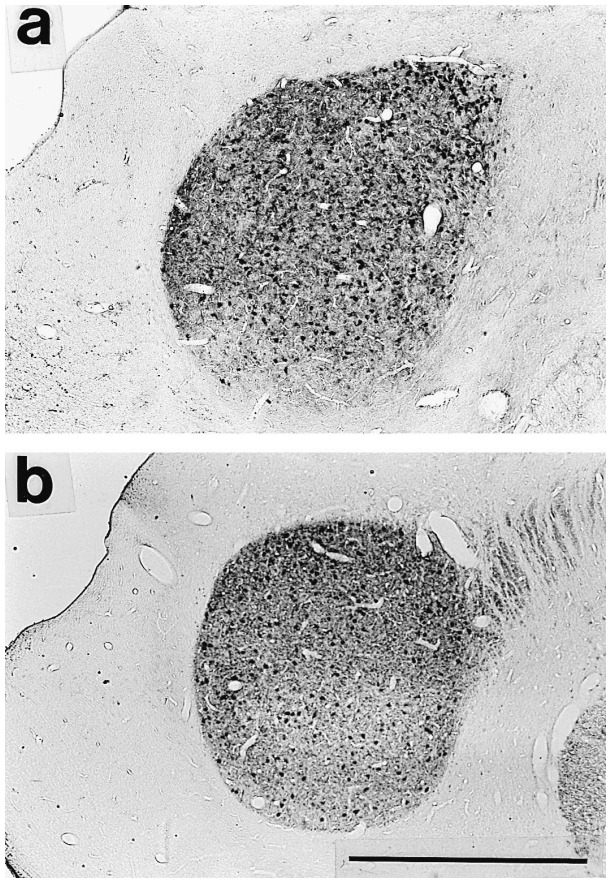

Fig. 7. Frontal sections of the left RT and T with Glu R4- (a) and PV-immunoreactive cells (b). Both antibodies resulted in staining of cell bodies and proximal parts of the stem dendrites, as well as strong labeling of neuropil. Bar = 1 mm.

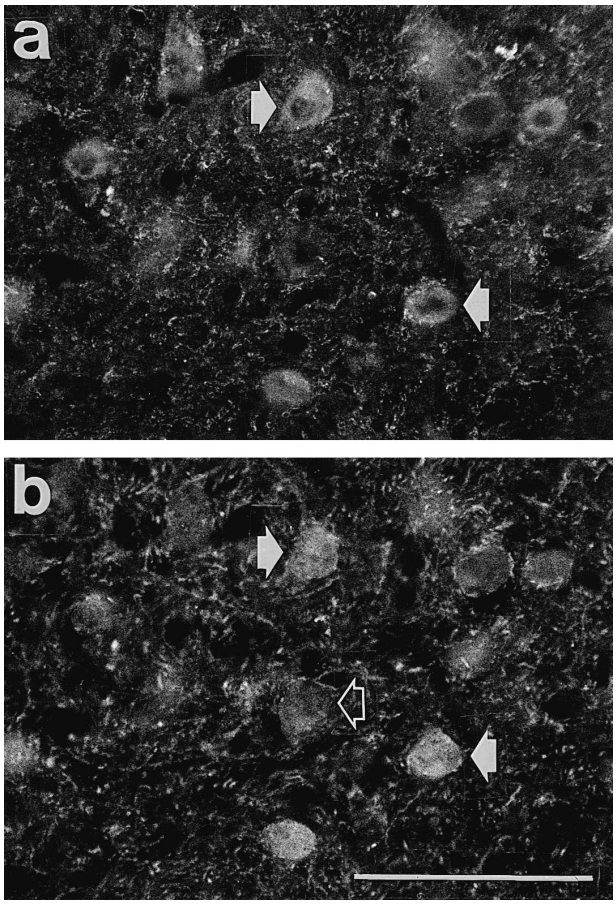

Fig. 8. Glu R4- (a) and PV- (b) like labeling in frontal sections of the rotundus. Glu R4 positive neurons (a, filled arrows) also expressed the PV-antigen (b, filled arrows). Additionally some PV-positive cells exhibited no Glu R4 co-expression (b, outlined arrow). Bar = 100 μm.

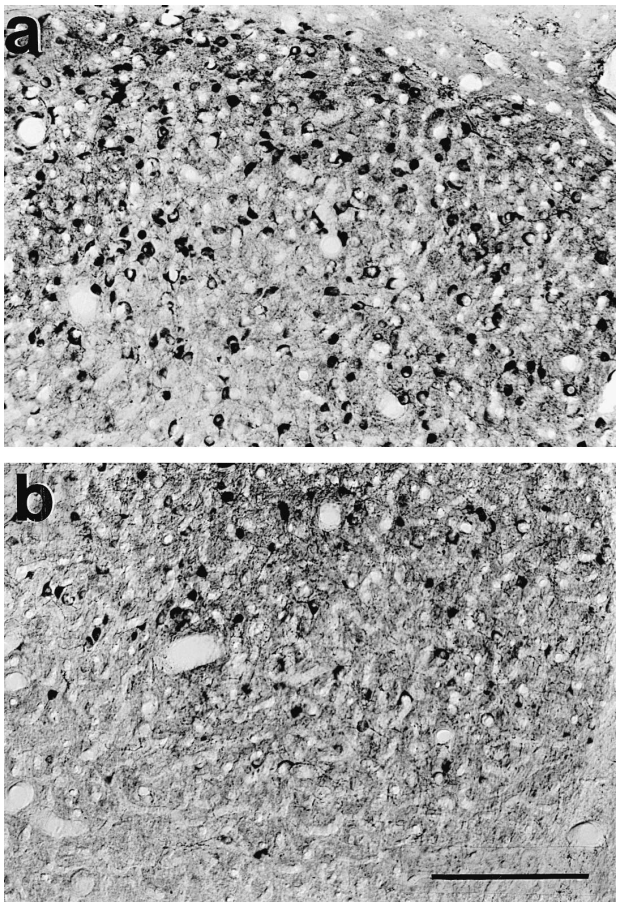

Fig. 10. Higher magnifications from the dorsal (a) and the ventral rotundus (b) of the same frontal section showing Glu R4-like immunoreactivity. Cell density decreased from dorsal to ventral. Bar = 250 μm.

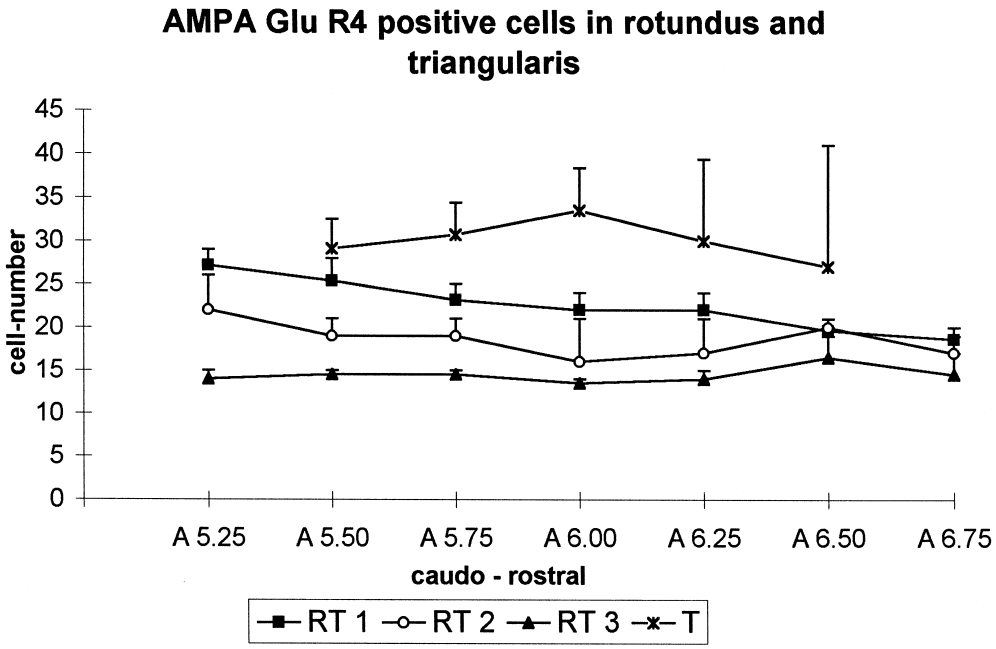

Fig. 9. Cell counts of Glu R4-positive neurons in the nuclei rotundus and triangularis showed a continuous increase in labeled cell numbers from dorsal (RT 1) to ventral (RT 3). Symbols indicate the mean cell numbers plus standard deviations. In the triangularis (T) the number of labeled cells was always slightly higher than in the rotundus.

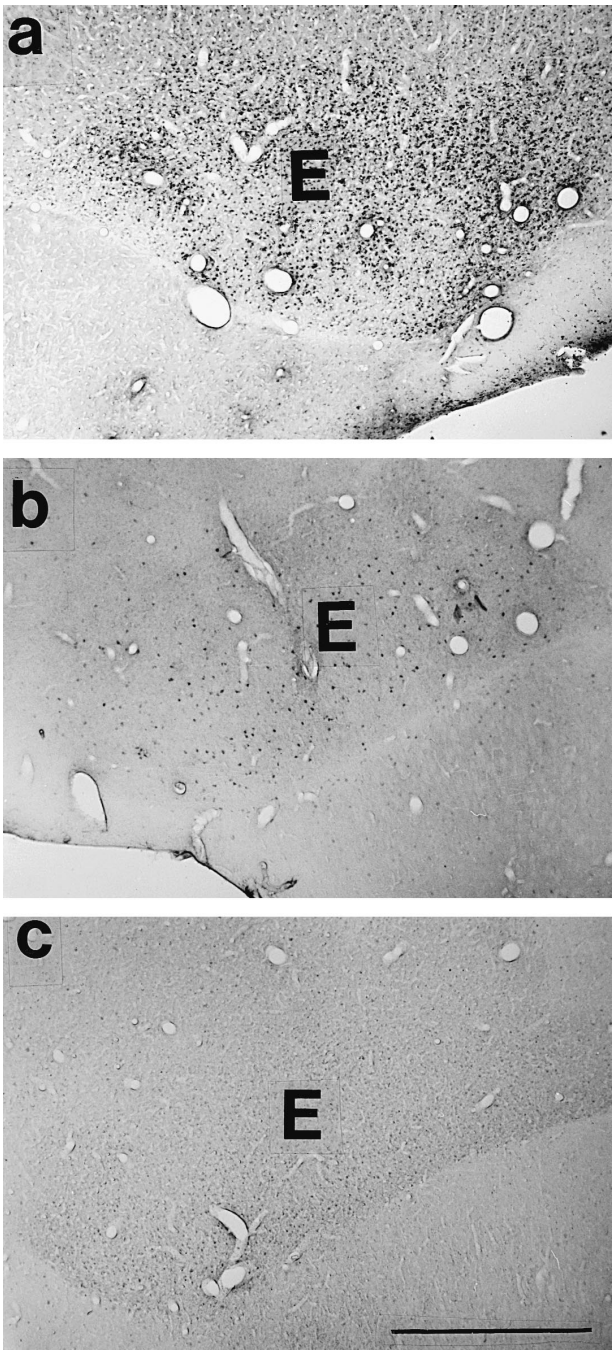

Fig. 11. Frontal sections throughout the right (a) or left (b, c) ectostriatum (E), stained against different glutamate-receptor subunits and parvalbumin. (a) The antibody to Glu R2/3 labeled somata and stem dendrites of a large number of cells, whereas (b) the antibody to Glu R4 marked only a few perikarya. (c) Parvalbumin-like immunoreactivity was nearly restricted to the ectostriatal neuropil. Bar = 1 mm.

revealed. Besides this glutamate-receptor positive neurons we found a moderate neuropil PV-immunoreactivity in this telencephalic structure (Fig. 11c). Additionally, a few clearly labeled PV-positive neurons could be observed. Double labeling experiments revealed them to be co-localised with Glu R2/3.

4. Discussion

The results of the present immunohistochemical study demonstrate that AMPA-receptors are expressed at all levels of the tectofugal system in the pigeon. Even if this investigations focus on AMPA-receptors, it is also conceivable that kainate- and NMDA-receptors are expressed in the tectofugal system, but up to know there is a lack of information on this receptor-expression. In the following paragraphs, the heterogeneous distribution of the AMPA-receptor subunits Glu R1, Glu R2/3, and Glu R4 along this ascending visual pathway is discussed, concerning their properties and functions in AMPA-receptors also referring to co-localisation with parvalbumin.

4.1. Tectum opticum

The present observation of AMPA-receptors within the optic tectum is in close correspondence with several previous studies which make it likely that the retinotectal system is at least partly glutamatergic. Glutamate uptake in the optic tectum is reduced after retinal ablations in chicks [7] and pigeons [36], while tectal release of glutamate is enhanced after optic nerve stimulation in pigeons [10]. Patch clamp studies in pigeons indicate glutamate to be the principle excitatory neurotransmitter in the retinotectal projection [18]. These data correspond to electrophysiological results in goldfish [46] and rat [67,70,71].

Together with a recent study [59], the present experiments revealed a Glu R1-positive horizontal band of cells in tectal layers 2 to 5 and a diffuse neuropil lamina in layers 4 to 7. Most of these labeled neurons seemed to be horizontal cells which are known to form triadic synaptic arrangements with their dendrites being post-synaptic to retinal input and pre-synaptic to the dendrites of radial neurons [3,32,64]. Due to the absence of other AMPA-receptor subunits in these layers, it is likely that retinal information is transmitted via homomeric Glu R1 receptors by horizontal cells. However, it is in principle also conceivable that the superficial Glu R1 neurophil labeling is expressed by tectal neurons of layers 9, 10, and 13, which receive retinal input by their superficially ramifying dendrites [39,60].

Glu R2/3 immunoreactivity was restricted to deeper layers 10 and 13, where mainly the perikarya of multipolar neurons were labeled. This staining pattern might indicate the existence of somatic glutamate-receptors with a glutamatergic axosomatic synaptic transmission. But also conceivable are dendritic or even pre-synaptically located AMPA-receptors on their axons. Due to the overlap of Glu R1 and a smaller contingent of Glu R2/3 somatic labeling it is conceivable that the synaptic input is mediated via heteromeric AMPA-receptors in at least a subpopulation of deep tectal neurons. A part of the input to these cells is

suspected to arise from radial tectal interneurons in layers 4, 9, and 11 which provide indirect retinal input to deep multipolar tectal cells [14]. In addition, several studies show that lamina 13 multipolar neurons are monosynaptically retinorecipient due to their superficially ascending dendrites [31,48,60,66].

The present results clearly revealed a significant dorso–ventral increase of 100% in the number of Glu R2/3 labeled cells of tectal layer 13. Since the same dorso–ventral gradient was observed in cresyl violet sections, it is not specific for Glu R2/3 labeled neurons, but reflects a general increase in cell number from dorsal to ventral. Several previous anatomical investigations had discovered additional dorso–ventral differentiations within the optic tectum of pigeons. Hayes and Webster [33] described a dorso–ventral division in the thickness of the retinorecipient layers 2–7 with an abrupt change at a borderline which roughly corresponds to the representation of the horizontal meridian. Additionally, dorso–ventral differences in the optic terminal density in layers 2–7, as well as in the number of synaptic contacts per terminal were shown [1,17]. The latter authors also demonstrated a differential cell morphology of intrinsic tectal neurons. Thus, the tectum is divided in a dorsal and a ventral component with a differing cytoarchitecture. The dorsal and ventral tectum also differ in connectivity. Tyrosine hydroxylase containing terminals within layer 4, 5a and 7 are concentrated within the dorsal tectum [69] while afferent inputs from the nucleus pretectalis to layer 5b and neuropeptide Y-positive fibers are predominant within the ventral tectal region [23,45]. Only this ventral area seems to project onto the retinopetal nucleus isthmo–opticus [13,87], while the ascending output to the n. geniculatus lateralis, pars dorsalis of the thalamofugal system mainly arises from the dorsal tectum [85]. Taken together these data imply fundamental dorso–ventral differences in the morphological architecture as well as the connectivity pattern of the optic tectum and raise questions regarding their functional implications.

It is conceivable that the tectal dorso–ventral variance is functionally related to the representation of the different retinal subfields. The pigeon's retina is divided into two fields based on the heterogeneous distribution of oil droplets located within the distal end of the inner cone segment. The red field in the dorso–temporal retina subserves fronto–ventral vision and is characterized by a large number of red and orange droplets. It is clearly separated from the remaining yellow field, which is characterized by a high density of yellow and greenish droplets, and which points into the lateral visual field [22]. While the representation of the retinal red field is located in the ventral half of the tectum, that of the area centralis is located at the area of transition [30,63]. Behavioural experiments make it likely that pigeons perceive and treat colour stimuli differently depending on them being perceived by the area centralis or by the red field [15,61]. Since one third of the tectal units have specific wavelength preferences [47] and since colour discrimination is mainly processed by the tectofugal system [26] these behavioural effects might hint to intratectal differences in colour processing. In addition, visual learning processes also seem to differ between stimuli seen with lateral or frontal vision. While visual discriminations learned using the red field are interocularly transferred, those learned with lateral vision are not [25]. Similarly, discriminations learned in the lateral field are intraocularly transferred to frontal vision, while the reverse transfer pattern is difficult to achieve [62,68]. A recent lesion study additionally shows that tectofugal lesions attenuate frontal but not lateral acuity [29]. These behavioural data make it likely that visual stimuli perceived by the area centralis or the red field are processed differently. It is conceivable that the dorso–ventral differentiation within the tectum might constitute a part of the anatomical substrate for this functional difference.

4.2. Rotundus and triangularis

Within the nuclei rotundus and triangularis the antibody against Glu R4 labeled a large number of neurons and produced a dense and specific neuropil staining. The rotundus is characterized by a predominance of multi-angular shaped relay neurons and some smaller interneurons [79]. Cell size measurements of immunoreactive cells revealed an unimodal distribution, indicating that only large relay neurons exhibited Glu R4-receptor subunits. However, since the proportion of interneurons seems to be extremely small [79] and their size overlaps with those of smaller relay neurons, it is presently not possible to decide whether interneurons in our sample were also Glu R4 labeled. The strong neuropil staining might be due to labeled dendritic processes expressing the receptor subunit Glu R4. Rotundal relay neurons were shown to develop extensive dendritic ramifications within 'terminal fields' throughout the entire rotundus, where they were observed to contact axon terminals of tecto–rotundal fibers [79]. Beside the indirect inhibitory tectal input via GABAergic neurons from the n. subpretectalis directed to the somata and apical dendrites of multi-angular neurons [56], the mayor afferent input to the rotundus arises from the tectum with diffuse termination zones within the rotundal matrix. The strong and homogeneous rotundal Glu R4 labeling observed in the present study makes glutamate as a key neurotransmitter of the tectorotundal projection very likely. As no further AMPA-receptor subunit labeling could be observed, it is likely that rotundal and triangular cells form homomeric glutamate receptors with Glu R4.

The quantitative analysis of rotundal Glu R4 positive and nissl-stained neurons revealed a heterogeneity, in which in three fields of measurement cell number decreased continuously from dorsal to ventral. In the triangularis cell density was slightly higher than in the rotundus. Up to now several studies described intrarotundal differentiations

based on histochemical, tract-tracing, and electrophysiological data. One common finding are dorso–ventral segregations, although some studies also showed rostro–caudal variations. The location as well as the total number of subdivisions vary widely between these publications. Granda and Yazulla [24] were the first to reveal dorso–ventral differences in the response patterns of rotundal units after tectal stimulations. The same authors could additionally reveal a subpopulation of colour sensitive cells which were restricted to the ventral rotundus. Also shapes of receptive fields [50] as well as the relative proportion of directionally sensitive neurons were reported to differ between dorsal and ventral rotundus [65]. Wang et al. [82] also subdivided the rotundus in dorso–ventrally oriented functional subfields. According to their data the ventral rotundus processes motion in 2D, whereas dorsal subfields show different response characteristics to stimulus features like colour, luminance and motion in depth. This differentiation is partly consistent with histochemical observations which demonstrated a dorso–ventral shift of acetylcholinesterase activity within the rotundus [49]. The ventral part of the rotundus is known to project exclusively onto the ventro–lateral ectostriatum while its dorsal components terminate within the rostral ectostriatum [5,55]. Afferents to the dorsally located triangularis as well as to the different intrarotundal subfields were described to arise from neurons located in different depths of tectal layer 13 [5].

Thus, all studies on the internal structure of the rotundus have observed dorso–ventrally oriented subdivisions. It is conceivable that distinct input patterns from tectal neurons located in different depths of layer 13 constitute the point of departure which ultimately leads to these intrarotundal subdivisions. The present data show that the functional and connectional differentiations within rotundus are accompanied by significant alterations in the number of relay neurons receiving direct tectal input via Glu R4-type glutamate-receptors.

4.3. Ectostriatum

In the ectostriatum a large number of AMPA Glu R2/3 positive neurons, and additionally some cells with AMPA Glu R4-like immunoreactivity were found. This is to our knowledge the first hint for a possible glutamatergic signal transmission in this telencephalic structure. In golgi preparations, large projection neurons and medium-sized interneurons could be distinguished within the ectostriatum [78]. On the basis of size measurements it is presently not possible to decide whether relay-, inter-, or both types of neurons express the AMPA-receptor subunits.

In an electronmicroscopic study, intraectostriatal terminals were categorized into three main groups, according to the shape of synaptic vesicles [83]. Only the spherical vesicle type was associated with asymmetric, and thus probably excitatory synapses, while the other two seemed to be involved in inhibitory signal transmission. So it is conceivable that Glu R2/3 and Glu R4 receptor subunits constitute a part of the post-synaptic complex in asymmetrical synapses containing spherical vesicles.

Within ectostriatal core and belt regions, neurons immunoreactive for glutamate-receptor subunits showed a comparable distribution and no differentiation was possible on the basis of their size and shape. This homogeneity of the AMPA-receptor labeling contrasts with electrophysiological evidences indicating ocular dominance bands within the ectostriatum [19,20]. Regional variations were also shown by histochemical demonstration of cytochrome-oxidase activity [34], which hints to regional differences in neuronal long term activity [86]. Thus, intraectostriatal subdivisions constituting ocular dominances and areas of differing long term activity seem not to be linked to the distribution of AMPA-receptor positive cells.

4.4. Physiological consequences of the heterogeneous AMPA-receptor distribution

With the antibodies directed against AMPA-receptor subunits it was not possible to distinguish between Glu R2 and Glu R3. In double-labeling experiments Glu R2/3- and Glu R4-positive neurons were examined for their co-expression with parvalbumin, which buffers calcium-influx and is probably the most potent intracellular calcium-binding protein. Parvalbumin was shown to be especially expressed in GABAergic inhibitory neurons [11], but is in some cases also present in glutamatergic cells [54].

Parvalbumin and Glu R4 were always found to be co-localized in rotundal neurons, probably indicating a calcium-permeability through this AMPA-receptor. In contrast the co-localisation of Glu R2/3 and parvalbumin varied along the tectofugal pathway. In the optic tectum no co-expression was observed, which can be a hint for calcium-impermeable AMPA-receptors, and thus to the presence of receptor-subunit Glu R2. In contrast, within the ectostriatum a small number of Glu R2/3 immunoreactive neurons also showed parvalbumin labeling. Since calcium impermeable glutamate-receptors require the receptor subunit Glu R2, a co-localisation of parvalbumin, which has a high affinity for calcium ions, and Glu R2 is unlikely within these cells. Thus, it is conceivable that some ectostriatal glutamate-receptors are homomeric for Glu R3, while the greater portion exhibit homomeric or heteromeric AMPA-receptors with the contribution of Glu R2.

Physiologically, the distinct distribution of post-synaptic AMPA-receptor subunits indicates different post-synaptic properties of the neurotransmitter, as for example only the expression of Glu R2 within a homomeric or heteromeric glutamate-receptor inhibits the calcium-influx. The calcium permeability of Glu R1-, Glu R3-, and Glu

R4-receptors and their heteromeric combinations is virtually on par with the calcium-permeability reported for NMDA-receptors [16,37]. So it is conceivable that AMPA-receptors which lack the Glu R2 subunit, and which therefore are able to mediate an increase in intracellular calcium concentration, might play a role in controlling synaptic plasticity [80]. This has already been demonstrated in an elegant electrophysiological study by Wall et al. [81] which showed alterations of activity patterns of rotundal units during the course of a classical heart-rate conditioning study.

5. Conclusions

The present study demonstrated a heterogeneous expression pattern of distinct AMPA-receptor subunits in the nuclei belonging to the tectofugal pathway. Different receptor subunits are characterized by unique properties, as for example AMPA Glu R2 determines the calcium influx through AMPA-receptors. Therefore, differences in the expression pattern indicate distinct physiological properties of glutamate in the ascending visual pathway.

AMPA-receptors in the superficial layers of the optic tectum are probably homomeric for Glu R1, while a heterogeneous structure with Glu R1 and Glu R2, and eventually Glu R3 is likely for neurons in the deeper layers. A dorso–ventral increase in layer 13 cell density makes a functional tectal segregation likely, which might be related to differences in the processing of inputs from the frontal and the lateral field of view. Additionally a dorso–ventral decrease in the cell number of probably homomeric Glu R4 AMPA-receptors was observed within the rotundus which probably represents different functional domains.

Acknowledgements

First of all we thank Karl Meller for his generous support, the sharing of his deep knowledge, and his helpful discussions during all aspects of the study. Thanks also to Martina Manns for all the prudent comments which were crucial in so many aspects, and Karl Donberg for his excellent technical assistance. Supported by the Deutsche Forschungsgemeinschaft (Gu 227/4-2) and the Alfred Krupp-Stiftung.

References

[1] D.W. Acheson, S.K. Kemplay, K.E. Webster, Quantitative analysis of optic terminal profile distribution within the pigeon optic tectum, Neuroscience 5 (1980) 1084–1967.

[2] J.C. Adams, Heavy metal intensification of DAB-based HRP reaction product, J. Histochem. Cytochem. 29 (1981) 775.

[3] P. Angaunt, J. Repérant, Fine structure of the optic fiber termination layers in the pigeon optic tectum: A Golgi and electron microscope study, Neuroscience 1 (1976) 93–105.

[4] P.M. Beart, An evacuation of L-glutamate as the transmitter released from optic nerve terminals of the pigeon, Brain Res. 110 (1976) 99–104.

[5] L.I. Benowitz, H.J. Karten, Organization of tectofugal visual pathway in pigeon: retrograde transport study, J. Comp. Neurol. 167 (1976) 503–520.

[6] H.J. Bischof, J. Niemann, Contralateral projection of the optic tectum in the zebra finch (*Taenopygia guttata castanotis*), Cell Tissue Res. 262 (1990) 307–313.

[7] S.C. Bondy, J.L. Purdy, Putative neurotransmitter of the avian visual pathway, Brain Res. 119 (1977) 417–426.

[8] J. Boulter, M. Hollmann, A. O'Shea-Greenfield, Molecular cloning and functional expression of glutamate receptor subunit genes, Science 249 (1990) 1033–1037.

[9] K. Braun, H. Scheich, M. Schachner, C.-W. Heizmann, Distribution of parvalbumin, cytochromoxidase activity and 14C-2-deoxyglucose uptake in the brain of the zebra finch: II. Visual system, Cell Tissue Res. 240 (1985) 117–127.

[10] V. Canzek, M. Wolfensberger, U. Amsler, M. Cuénod, In vivo release of glutamate and aspartate following optic nerve stimulation, Nature 293 (1981) 572–574.

[11] M.R. Celio, Parvalbumin in most gamma-aminobutyric acid-containing neurons in the rat cerebral cortex, Science 231 (1986) 995–997.

[12] M.R. Celio, W. Baier, L. Scharer, P.A. de Viragh, C. Gerday, Monoclonal antibodies directed against the calcium binding protein parvalbumin, Cell Calcium 9 (1988) 81–86.

[13] P.G. Clarke, M. Gyger, S. Catsicas, A centrifugally controlled circuit in the avian retina and its possible role in visual attention switching, Vis. Neurosci. 13 (1996) 1043–1048.

[14] M. Cuénod, P. Streit, Amino acid transmitters and local circuitry in optic tectum, in: F.O. Schmitt, F.G. Worden (Eds.), The neurosciences fourth study program. MIT Press, Cambridge, 1979, pp. 989–1004.

[15] J.D. Delius, E. Jahnke-Funk, A. Hawker, Stimulus display geometry and colour discrimination learning by pigeons, Curr. Psych. Res. 1 (1981) 203–214.

[16] R. Dingledine, R.I. Hume, S. Heinemann, Structural determinants of barium permeation and rectification in non-NMDA glutamate receptor channels, J. Neurosci. 12 (1992) 4080–4087.

[17] T.A. Duff, G. Scott, R. Mai, Regional differences in pigeon optic tract, chiasm, and retino-receptive layers of optic tectum, J. Comp. Neurol. 198 (1981) 231–247.

[18] J.C. Dye, H.J. Karten, An in vitro study of retinotectal transmission in the chick: role of glutamate and GABA in evoked field potentials, Vis. Neurosci. 13 (1996) 747–758.

[19] J. Engelage, H.J. Bischof, Enucleation enhances ipsilateral flash evoked responses in the ectostriatum of the zebra finch (*Taeniopygia guttata castanotis* Gould), Exp. Brain Res. 70 (1988) 79–89.

[20] J. Engelage, H.J. Bischof, Flash evoked potentials in the ectostriatum of the zebra finch: a current source–density analysis, Exp. Brain Res. 70 (1989) 79–89.

[21] G.E. Fagg, L-Glutamate, excitatory amino acid receptors and brain function, Trends Neurosci. 8 (1985) 207–210.

[22] Y. Galifret, The various functional areas of the retina of pigeons, Z Zellforsch. Mikrosk. Anat. 86 (1968) 535–545.

[23] P.D. Gamlin, A. Reiner, K.T. Keyser, N. Brecha, H.J. Karten, Projection of the nucleus pretectalis to a retinorecipient tectal layer in the pigeon (*Columba livia*), J. Comp. Neurol. 368 (1996) 424–438.

[24] A.M. Granda, S. Yazulla, The spectral sensitivity of single units in the nucleus rotundus of pigeon, *Columba livia*, J. Gen. Physiol. 57 (1971) 363–384.

[25] M.A. Goodale, J.A. Graves, Interocular transfer in the pigeon: retinal locus as a factor, Adv. in Anal. of Vis. Behav. Ingle. MIT Press, 1982.

[26] O. Güntürkün, The functional organization of the avian visual system, in: R.J. Andrew (Ed.), Neural and Behavioural Plasticity: The use of the domestic chick as a model. Oxford Univ. Press, 1991, pp. 92–105.
[27] O. Güntürkün, Vision, in: G.C. Whittow (Ed.), Sturkie's Avian Physiology, Academic Press, Orlando, in press.
[28] O. Güntürkün, G. Melsbach, W. Hörster, S. Daniel, Different sets of afferents are demonstrated by the two fluorescent tracers Fast Blue and Rhodamine, J. Neurosci. Meth. 49 (1993) 103–111.
[29] U. Hahmann, Ph.D. thesis, Bochum, 1994.
[30] F.A. Hamdi, D. Whitteridge, The representation of the retina on the optic tectum of the pigeon, Q. J. Exp. Psychol. 39 (1954) 111–119.
[31] O. Hardy, N. Leresche, D. Jassik-Gerschenfeld, Morphology and laminar distribution of electrophysiologically identified cells in the pigeon's optic tectum: an intracellular study, J. Comp. Neurol. 233 (1985) 390–404.
[32] B.P. Hayes, K.E. Webster, An electron microscope study of the retino-receptive layers of the pigeon optic tectum, J. Comp. Neurol. 162 (1975) 447–466.
[33] B.P. Hayes, K.E. Webster, Cytoarchitectural fields and retinal termination: an axonal transport study of laminar organization in the avian optic tectum, Neuroscience 16 (1985) 641–657.
[34] B. Hellmann, C. Waldmann, O. Güntürkün, Cytochrome oxidase activity reveals parcellations of the pigeon's ectostriatum, Neuroreport 6 (1995) 881–885.
[35] H. Henke, T.M. Schenker, M. Cuénod, Uptake of neurotransmitter candidates by pigeon optic tectum, J. Neurochem. 26 (1976) 125–130.
[36] H. Henke, T.M. Schenker, M. Cuénod, Effects of retinal ablation on uptake of glutamate, glycine, GABA, proline and choline in pigeon tectum, J. Neurochem. 26 (1976) 131–134.
[37] M. Hollmann, S. Heinemann, Cloned glutamate receptors, Ann. Rev. Neurosci. 17 (1994) 31–108.
[38] M. Hollmann, A. O'Shea-Greefield, S.W. Rogers, S. Heinemann, Cloning by functional expression of a member of the glutamate receptor family, Nature 342 (1989) 643–648.
[39] S.P. Hunt, H. Künzle, Observations on the projections and intrinsic organization of the pigeon optic tectum: an autoradiographic study based on anterograde and retrograde, axonal and dendritic flow, J. Comp. Neurol. 170 (1976) 153–172.
[40] H.J. Karten, W. Hodos, A stereotaxic atlas of the brain of the pigeon, Baltimore, Johns Hopkins Press, 1967.
[41] H.J. Karten, W. Hodos, Telencephalic projections of the nucleus rotundus in the pigeon (*Columba livia*) , J. Comp. Neurol. 140 (1970) 35–52.
[42] H.J. Karten, A.M. Revzin, The afferent connections of the nucleus rotundus in the pigeon, Brain Res. 2 (1966) 368–377.
[43] H.J. Karten, T. Shimizu, The origins of neocortex: Connections and laminations as distinct events in evolution, J. Cog. Neurosci. 1 (1989) 291–301.
[44] K. Keinänen, W. Wisden, B. Sommer, A family of AMPA-selective glutamate receptors, Science 249 (1990) 556–560.
[45] W. Kuenzel, S. Blahser, Vasoactive intestinal polypeptide (VIP)-containing neurons: distribution throughout the brain of the chick (*Gallus domesticus*) with focus upon the lateral septal organ, Cell Tissue Res. 275 (1994) 91–107.
[46] R.B. Langdon, J.A. Freeman, Antagonists of glutaminergic neurotransmission block retinotectal transmission in goldfish, Brain Res. 398 (1986) 169–174.
[47] J. Letelier, Respuestas comáticas en el tectum óptico de la paloma. Tesis de Licenciatura, Fakultad de Ciencias, Universitad de Chile, Santiago, Chile, 1983.
[48] H. Luksch, K. Cox, H.J. Karten, Morphology and connectivity of neurons in the chick tectofugal visual pathway: implications on function and evolution, Proc. 25th Göttingen Neurobiology Conference, Vol. 2, 1997, p. 534.
[49] M. Martinez-de-la-Torre, S. Martinez, L. Puelles, Acetylcholinesterase-histochemical differential staining of subdivisions within the nucleus rotundus in the chick, Anat. Embryol. 181 (1990) 129–135.
[50] J.H. Maxwell, A.M. Granda, Functional localisation in the nucleus rotundus, in: A.M. Granda, J.H. Maxwell (Eds.), Neural Mechanisms of Behavior in the Pigeon, Plenum, NY, 1979, pp. 165–175.
[51] M.L. Mayer, G.L. Westbrook, Permeation and block of *N*-methyl-D-aspartic acid receptor channels by divalent cations in mouse cultured central neurons, J. Physiol. London 394 (1987) 501–527.
[52] D. McCormick, Neurotransmitter actions in the thalamus and cerebral cortex and their role in neuromodulation of thalamo–cortical activity, Prog. Neurobiol. 39 (1992) 337–388.
[53] D.T. Monaghan, R.J. Bridges, C.W. Cotman, The excitatory amino acid receptors: their classes, pharmacology, and distinct properties in the function of the central nervous system, Ann. Rev. Pharmacol. Toxicol. 29 (1989) 365–402.
[54] C. Nitsch, P. Maly, D. Möri, A.L. Scotti, Evidence for the co-localisation of parvalbumin and glutamate, but not GABA, in the perforant path of the gerbil hippocampal formation: a combined immunocytochemical and microquantitative analysis, J. Neurochem. 62 (1994) 1276–1284.
[55] B.E. Nixdorf, H.J. Bischof, Afferent connections of the ectostriatum and visual wulst in the zebrafinch (*Taeniopygia guttata castanotis* Gould)—an HRP study, Brain Res. 248 (1982) 9–17.
[56] T.D. Ngo, A. Nemeth, T. Tömböl, Some data on GABA-ergic innervation of nucleus rotundus in chicks, J. Hirnfosch. 33 (1992) 335–355.
[57] T.D. Ngo, D.C. Davies, G.Y. Egedi, T. Tömböl, A phaseolus lectin anterograde tracing study of the tectorotundal projections in the domestic chick, J. Anat. 184 (1994) 129–136.
[58] H.P. Ottiger, A. Gerfin-Moser, F. Del Principe, F. Dutly, P. Streit, Molecular cloning and differential expression patterns of avian glutamate receptor mRNAs, J. Neurochem. 64 (1995) 2413–2426.
[59] R.S. Pires, L.R.G. Britto, Distribution of AMPA-type glutamate receptor subunits in the chick visual system, Baz. J. Med. Biol. Res. 30 (1997) 73–77.
[60] S. Ramon y Cajal, Histologie du Système Neveux de l'Homme et des Vertébrés, Vol. 2, Maloine, Paris, 1911.
[61] M. Remy, J. Emmerton, Behavioral spectral sensitivities of different retinal areas in pigeons, Behav. Neurosci. 103 (1989) 170–177.
[62] M. Remy, J. Emmerton, Directional dependence of intraocular transfer of stimulus detection in pigeons (*Columba livia*), Behav. Neurosci. 105 (1991) 647–652.
[63] M. Remy, O. Güntürkün, Retinal afferents to the tectum opticum and the n. opticus principalis thalami in the pigeon, J. Comp. Neurol. 305 (1991) 57–70.
[64] J. Repérant, P. Angaut, The retinotectal projections in the pigeon. An experimental optical and electron microscope study, Neuroscience 2 (1977) 119–140.
[65] A.M. Revzin, Functional localisation in the nucleus rotundus, in: A.M. Granda, H.J. Maxwell (Eds.), Neural Mechanisms of Behavior in the Pigeon, Plenum, NY, 1979, pp. 165–175.
[66] F. Ris, Über den Bau des Lobus opticus der Vögel, Arch. Mikros. Anat. Entwicklgsg. 53 (1899) 106–130.
[67] W.A. Roberts, S.A. Eaton, T.E. Salt, Excitatory amino acid receptors mediate synaptic responses to visual stimuli in superior colliculus neurons of the rat, Neurosci. Lett. 129 (1991) 161–164.
[68] W.A. Roberts, M.T. Phelps, T. Macuda, D.R. Brodbeck, T. Russ, Intraocular transfer and simultaneous processing of stimuli presented in different visual fields of the pigeon, Behav. Neurosci. 110 (1996) 290–299.
[69] H.R. Rodman, H.J. Karten, Laminar distribution and sources of catecholaminergic input to the optic tectum of the pigeon (*Columba livia*), J. Comp. Neuro. 359 (1995) 424–442.
[70] T. Sakurai, T. Miyamoto, Y. Okada, Reduction of glutamate content in rat superior colliculus after retino–tectal denervation, Neurosci. Lett. 109 (1990) 299–303.

[71] T. Sakurai, Y. Okada, Selective reduction of glutamate in rat superior colliculus and dorsal lateral geniculate nucleus after contralateral enucleation, Brain Res. 573 (1992) 197–203.
[72] M.E. Schneider, A.S. Niedzielski, R.J. Wenthold, AMPA receptors from the chick brain, Soc. Neurosci. Abstr. 18 (1992) 259.
[73] M.E. Schneider, AMPA receptors from the chick cochlear ganglion, A.R.O. Abstr. 17 (1994) 139.
[74] S.Y. Shu, The glucose oxidase–DAB–nickel method in peroxidase histochemistry of the nervous system, Neurosci. Lett. 85 (1988) 169–171.
[75] F. Sladeczek, J.P. Pin, M. Recasens, J. Bockaert, S. Weiss, Glutamate stimulates inositol phosphate formation in striatal neurons, Nature 317 (1985) 717–719.
[76] H. Sugiyama, I. Ito, C. Hirono, A new type of glutamate receptor linked to inositol phospholipid metabolism, Nature 325 (1987) 531–533.
[77] R. Tinner, M. Oertle, C.W. Heizmann, H.R. Bosshard, Calcium-binding site of carp parvalbumin recognized by monoclonal antibody, Cell Calcium 11 (1990) 19–23.
[78] T. Tömböl, Z. Magloczky, M.G. Stewart, A. Csillag, The structure of chicken ectostriatum: I. Golgi study, J. Hirnforsch. 29 (1988) 525–546.
[79] T. Tömböl, T.D. Ngo, G. Egedy, EM and EM golgi study on structure of nucleus rotundus in chicks, J. Hirnforsch. 33 (1992) 215–234.
[80] P. Vanderklish, R. Neve, B.A. Bahr, A. Arai, M. Hennegriff, J. Larson, G. Lynch, Translational suppression of a glutamate receptor subunit impairs long-term potentiation, Synapse 12 (1992) 333–337.
[81] J.T. Wall, C.M. Gibbs, J.L. Broyles, D.H. Cohen, Modification of neuronal discharge along the ascending tectofugal pathway during visual conditioning, Brain Res. 342 (1985) 67–76.
[82] Y. Wang, S. Jiang, B.J. Frost, Visual processing in pigeon nucleus rotundus: luminance, colour, motion, and looming subdivisions, Vis. Neurosci. 10 (1993) 21–30.
[83] M. Watanabe, H. Ito, M. Ikushima, Cytoarchitecture and ultrastructure of the avian ectostriatum: afferent terminals from the dorsal telencephalon and some nuclei in the thalamus, J. Comp. Neurol. 236 (1985) 241–257.
[84] J.C. Watkins, R.H. Evans, Excitatory amino acid transmitters, Ann. Rev. Pharmacol. 21 (1981) 165–204.
[85] J.M. Wild, Vestibular projections to the thalamus of the pigeon: an anatomical study, J. Comp. Neurol. 271 (1988) 451–460.
[86] M. Wong-Riley, Changes in the visual system of monocularly sutured or enucleated cats demonstrable with cytochrome oxidase histochemistry, Brain Res. 171 (1979) 11–28.
[87] W. Woodson, T. Shimizu, J.M. Wild, J. Schimke, K. Cox, H.J. Karten, Centrifugal projections upon the retina: an anterograde tracing study in the pigeon (*Columba livia*), J. Comp. Neurol. 362 (1995) 489–509.